

4-12-2022

Symmetric Neutrosophic Cross Entropy Based Fault Recognition of Turbine

Chander Parkash

Follow this and additional works at: https://digitalrepository.unm.edu/nss_journal

Recommended Citation

Parkash, Chander. "Symmetric Neutrosophic Cross Entropy Based Fault Recognition of Turbine." *Neutrosophic Sets and Systems* 49, 1 (2022). https://digitalrepository.unm.edu/nss_journal/vol49/iss1/19

This Article is brought to you for free and open access by UNM Digital Repository. It has been accepted for inclusion in *Neutrosophic Sets and Systems* by an authorized editor of UNM Digital Repository. For more information, please contact disc@unm.edu.



Symmetric Neutrosophic Cross Entropy Based Fault Recognition of Turbine

Chander Parkash*¹

¹Department of Mathematics, Rayat Bahra University, Mohali, Punjab, India. Email: cpgandhi@rayatbahrauniversity.edu.in

*Correspondence: cchanderr@gmail.com

Abstract: This study introduces a novel fault recognition methodology for turbine faults through symmetric trigonometric fuzzy and neutrosophic cross entropy measures (FCEM and NCEM) consequently. After knowing the nethermost (lowest) and uppermost (highest) energy bounds of each real fault conditions, the energy interval ranges are constructed and then transformed into the form of single valued neutrosophic (SN) sets. Thereafter, the proposed symmetric trigonometric cross -entropy measures are deployed to recognize faults of turbine. The nethermost FCEM and NCEM values between familiar and unfamiliar fault conditions indicates that the unfamiliar fault condition is closer to the familiar one. The applicability of the proposed methodology is validated by taking into consideration the example of fault diagnosis of turbine. The repercussions of this study yield that the proposed symmetric trigonometric FCEM and NCEM cannot only recognize optimal fault, they can also provide meaningful and remarkable fault information. A comparison of the underlying FCEM and NCEM (based on SN sets) with the enduring cosine measures (based on vague sets) conclude that the latter sets may hide some fruitful fault information., when experimented under sensitive and intuitive criteria and thus resulting an incomplete fault evaluation criterion.

Keywords: Fuzzy Sets, Neutrosophic Sets, Cross Entropy, Fault Diagnosis, Turbine.

1. Introduction

A Turbine generator is an important mechanical device and is being widely used for converting heat energy of steam into electrical energy in thermal plants. It is a natural process for a huge steam turbine generator to have vibrations produced by many factors such as misalignment, heating of rotor element and lubricant oil etc. When a fault occurs, it not only damages the generator set but also disturbs the continuous and safe operation of internal machinery. Careful analysis of vibration signals of the generator set can reveal some useful evaluation information, which in turn, can avoid catastrophic mechanical disorder as well as huge economic losses. It is, therefore, necessary to reckon and fix the actual cause of the fault as early as possible. Over the past few years, researchers have developed some fault recognition methods, that works on cross entropy measures, for quantifying the non-linear relationship between unfamiliar and familiar turbine fault conditions. Recently, Ren et al. [1] extracted the fuzzy entropy of a series of mode components for observing the complexity of working condition and thereafter improved the fault diagnosis accuracy of wind

turbine. Lilian and Ye [2,3] modified the vague sets of enduring similarity measure and observed the non-linear and complex relationship between vibration signals and various fault conditions. Recently, Lilian Shi [4] constructed simplified neutrosophic sets by exercising the enduring Karl Pearson's coefficient of correlation and combined it with wavelet packet transforms for reckoning faults of rolling bearing. Tian et al. [5] established a systematic and comprehensive approach based on permutation entropy for automatic testimony of bearing defects under and time varying conditions. Recently, Martinez et al. [6] utilized Shannon's Information entropy for quantifying and extracting the fault information available in the vibration signals of broken bars in induction motors. Under multi fault severities and time-varied complexities, Fu et al. [7] combined approximate entropy and wavelet packet transforms for decomposing deterministic and stochastic power signals. Zhao et al. [8] extended the existing wavelet entropy to instantaneous wavelet singular entropy for extracting the sensor fault characteristics of a gas turbine. Zhao et al. [8] deployed multiscale fuzzy distribution entropy for understanding the nonlinear and non-consistent fault characteristics signals. Zhang et al. [9] understood the irregularity and complexity of vibration signals by extending Shannon's entropy to wavelet entropy and concluded that whenever wavelet entropy increases, the tightness conditions of bolted joints diverge to looseness. Leite et al. [10] deployed Shannon's entropy and Jensen-Renyi's directed divergence (JRDD) for constructing discrete probability mass function of a known time waveform and utilized it for identifying faults of rolling bearing elements. Many times, the approaches based on variants of Shannon's probabilistic entropy and JRDD have been found inefficacious in providing semantic output due to the difficulty in transforming fault characteristics of cumbersome signals. Hence, the above-mentioned fault diagnosis techniques may not be capable for extracting remarkable and accurate fault information from faults conditions of turbine. This reinforces the exigency for an effective fault diagnosis procedure which can make precise and fruitful analysis for a fault that occurs in turbine generator set because the same symptom of a fault may have variety of fault causations. A single valued neutrosophic (SN) set [11] is mainly portrayed by truth, indeterminacy and falsity membership functions and inherits its indeterminacy into the form of truth and falsity values. Kumar et al. [12,13] effectively identified bearing faults by decomposing vibrational signals

into eight different frequency modes under neutrosophic environment. However, the enduring research on neutrosophic sets and systems have mainly dealt with its theoretical or asymmetrical aspects and ignores those engineering problems which may exhibit symmetrical phenomenon or return inconsequential results under neutrosophic treatments. Neutrosophic cross entropy approach has been found significantly efficacious in tackling complex engineering problems under multi-faults severities. Till so far, no symmetric neutrosophic cross entropy measure has been developed and utilized for improving fault identification accuracy of turbine. Subsequently, an effort is accomplished in this direction which can overcome the above-mentioned shortcomings and effectively diagnose the faults of a huge steam turbine generator set. Moreover, the underlying symmetric trigonometric cross entropy measure of neutrosophic sets provides meaningful fault information whereas the enduring similarity measure may hide some fruitful fault information and thus resulting an ambiguous phenomenon. In addition,

Section 2 deals with pre-requisites of neutrosophic entropy measure, needed for the successive growth of the proposed research. **Section 3** is devoted to establish a novel symmetric trigonometric FCEM whereas **Section 4** expands the outcomes of **Section 3** to another novel symmetric cross entropy measure, hinged on two single valued neutrosophic sets. **Section 5** inaugurates the proposed neutrosophic cross entropy-based fault recognition methodology, the applicability and remarkability of which are exemplified in **Section 6**. Finally, **Section 6** contributes the concrete conclusions extracted from this study.

2. Preliminaries: -

This section deals with the introduction of some familiar apprehensions as follows:

Def. 2.1 SN Entropy Measure [11-13] A SN set, in any universal set X with its generic elements x_1, x_2, \dots, x_n , is an entity of the form: $A = \langle x_i, \mu_A(x_i), i_A(x_i), f_A(x_i) \mid x_i \in X \rangle$ where each $\mu_A(x_i): X \rightarrow [0,1], i_A(x_i): X \rightarrow [0,1], f_A(x_i): X \rightarrow [0,1]$ satisfy $0^- \leq \mu_A(x_i) + i_A(x_i) + f_A(x_i) \leq 3^+$. Suppose $T(X)$ represents the collection of all SN sets in X , Then $T_N(A): T(X) \rightarrow R$ is called as SN entropy measure if

(i) $T_N(A) \geq 0 \forall 0 \leq \mu_A(x_i), i_A(x_i), f_A(x_i) \in [0,1]$ with equality if either $\mu_A(x_i) = 1, i_A(x_i) = 0, f_A(x_i) = 0$ or $\mu_A(x_i) = 0, i_A(x_i) = 0, f_A(x_i) = 1$. (ii) $T_N(A^c) = T_N(A)$. If A^c denotes the complement of A , then $A^c = (\langle x_i, f_A(x_i), 1 - i_A(x_i), \mu_A(x_i) \rangle | x_i \in X)$.

(iii) $T_N(A)$ possesses concavity property for each $\mu_A(x_i), i_A(x_i), f_A(x_i)$.

(iv) $T_N(A)$ admits its maximum value which arises when $\mu_A(x_i) = i_A(x_i) = f_A(x_i) = \frac{1}{2}$.

3. A Novel Symmetric Trigonometric FCEM (Fuzzy Cross Entropy Measure)

We first establish the following **Theorem 3.1**, the out coming of which will be a backbone for the proposed symmetric trigonometric fuzzy cross entropy measure, hinged on two fuzzy sets (**Theorem 3.2**).

Theorem.3.1 Set $T_0 = \sqrt{\mu_A(x_i)}, T_1 = \sqrt{1 - \mu_A(x_i)}, T_2 = \sqrt{\mu_A(x_i)(1 - \mu_A(x_i))}$. Let $A \subseteq X$ be any fuzzy set [14]. Then

$$T_{FS}(A) = \sum_{i=1}^n \left[\tan\left(\frac{3\sqrt{2}}{3\sqrt{2}+2}\right) - \tan\left(\frac{3\sqrt{2}}{3\sqrt{2}+2(T_0+T_1)-\sqrt{2}T_2}\right) \right] \dots (1)$$

represents a valid measure of fuzzy entropy with $Max.T_{FS}(A) = \left(\tan\frac{3\sqrt{2}}{3\sqrt{2}+2} - \tan\frac{2}{3}\right)n$ and minimum value as zero.

Proof (i) The expressions denoted by T_0, T_1, T_2 are non0negative because $\mu_A(x_i) \in [0,1]$. This justifies that $T_F(A) \geq 0 \forall \mu_A(x_i) \in [0,1]$ with equality $T_0 = 0, T_1 = 1, T_2 = 1$ or $T_0 = 1, T_1 = 0, T_2 = 0$. In other words, $T_F(A)$ vanishes whenever $\mu_A(x_i) = 0$ or 1 .

(ii) If we replace $\mu_A(x_i)$ with its counterpart $1 - \mu_A(x_i)$, then T_0 changes to T_1 , $T_1 \rightarrow T_0, T_2 \rightarrow T_2$, which means $T_F(A^c) = T_F(A)$.

(iii) **Concavity:** To establish the concavity of $T_{FS}(A)$, differentiating (1) partially with respect to $\mu_A(x_i)$ to get

$$\frac{\partial T_{FS}(A)}{\partial \mu_A(x_i)} = \frac{3\sqrt{2} \left(\frac{T_1^2 - T_0^2}{T_0 T_1 (T_0 + T_1)} - \frac{1 - 2T_0^2}{\sqrt{2} T_2} \right) \sec^2 \frac{3\sqrt{2}}{3\sqrt{2} + 2(T_0 + T_1) - \sqrt{2} T_2}}{(3\sqrt{2} + 2(T_0 + T_1) - \sqrt{2} T_2)^2} \dots (2)$$

It is informative to point out that $T_1^2 - T_0^2 = 1 - 2\mu_A(x_i) = 1 - 2T_0^2$. With this information in hand, the above equality simplifies to

$$\frac{\partial T_{FS}(A)}{\partial \mu_A(x_i)} = \frac{3\sqrt{2}(1 - 2\mu_A(x_i)) \left(\frac{1}{T_0 T_1 (T_0 + T_1)} - \frac{2}{\sqrt{2} T_2} \right) \sec^2 \frac{3\sqrt{2}}{3\sqrt{2} + 2(T_0 + T_1) - \sqrt{2} T_2}}{(3\sqrt{2} + 2(T_0 + T_1) - \sqrt{2} T_2)^2} \dots (3)$$

Again, partial differentiation of (2) with respect to $\mu_A(x_i)$ yields

$$\frac{\partial^2 T_{FS}(A)}{\partial \mu_A^2(x_i)} = \frac{9 \left[\frac{(\sqrt{2} - 2T_1 + 2T_1 T_0^2 - 2T_0^3)(3\sqrt{2} + 2T_1 + 2T_0 - \sqrt{2} T_2)^2}{2\sqrt{2} T_1 (T_0^2 - 1) T_0^3} + \left(\frac{1}{T_0} - \frac{1}{T_1} - \frac{1 - 2T_0^2}{\sqrt{2} T_2} \right)^2 \left(\frac{2\sqrt{2}(3\sqrt{2} + 2(T_0 + T_1) - \sqrt{2} T_2)}{3\sqrt{2} + 2(T_0 + T_1) - \sqrt{2} T_2} + 12 \tan \frac{3\sqrt{2}}{3\sqrt{2} + 2(T_0 + T_1) - \sqrt{2} T_2} \right) \right] \sec^2 \frac{3\sqrt{2}}{3\sqrt{2} + 2(T_0 + T_1) - \sqrt{2} T_2}}{(3\sqrt{2} + 2(T_0 + T_1) - \sqrt{2} T_2)^2} \leq 0$$

for each $\mu_A(x_i) \in [0, 1]$, This establishes that $T_{FS}(A)$ exhibits the concavity property with respect to $\mu_A(x_i)$. This motivates $T_F(A)$ to admit its maximum value which can occur if $\frac{\partial T_{FS}(A)}{\partial \mu_A(x_i)} = 0$ and

hence (1) yields $\mu_A(x_i) = \frac{1}{2}$. Thus,

$$\text{Max. } T_{FS}(A) = T_{FS}(A) \Big|_{\mu_A(x_i) = \frac{1}{2}} = \left(\tan \frac{3\sqrt{2}}{3\sqrt{2} + 2} - \tan \frac{2}{3} \right) n. \dots (4)$$

Also, the graphical representation of $T_{FS}(A)$ as shown in Fig 2 justifies that it admits its minimum value as zero.

Theorem.3.2 Set $E_0 = \sqrt{\mu_B(x_i)}, E_1 = \sqrt{1 - \mu_B(x_i)}$. Let A and B belongs to $T(X) \times X$, then $T_{FS}^\mu(A, B)$ is a correct symmetric trigonometric FCEM (fuzzy cross entropy measure [15-16]) given as

$$\begin{aligned}
 & T_{FS}^\mu(A, B) \\
 &= \sum_{i=1}^n \left[-6 \tan\left(\frac{2}{3}\right) + (2 + T_0^2 + E_0^2) \tan\left(\frac{2 + T_0^2 + E_0^2}{3 + 2(T_0 + E_0)\sqrt{\frac{T_0^2 + E_0^2}{2}} - T_0 E_0}\right) + (4 - T_0^2 - E_0^2) \tan\left(\frac{4 - T_0^2 - E_0^2}{3 + 2(T_1 + E_1)\sqrt{\frac{2 - T_0^2 - E_0^2}{2}} - T_1 E_1}\right) \right] \dots (5)
 \end{aligned}$$

Here, $T_{FS}^\mu(A, B)$ represents the subjective value of symmetric discrimination of A against B .

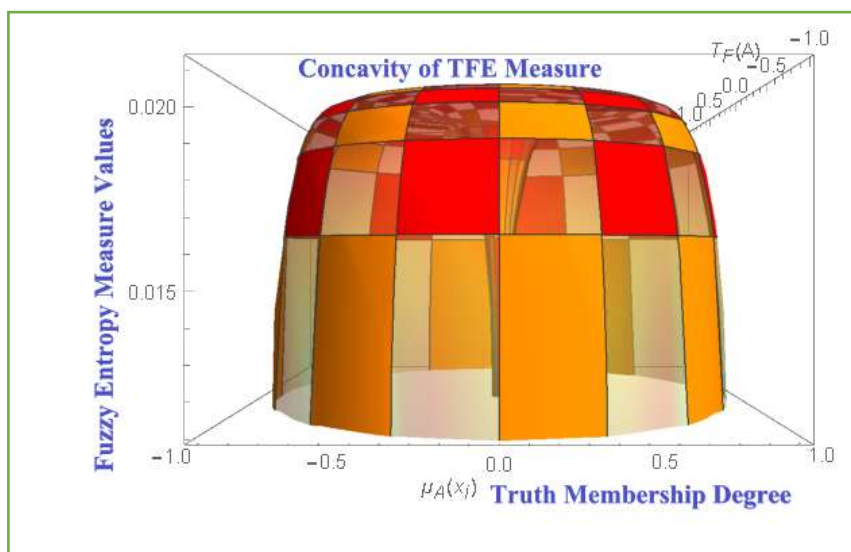


Fig. 2 A Revolution Plot for the Concavity Property and Minimum value of $T_{FS}(A)$

Proof. (i) Since $T_{FS}^\mu(A, B)$ does not change after the replacement of $\mu_A(x_i)$ with $\mu_B(x_i)$, this validates the symmetric nature of $T_{FS}^\mu(A, B)$.

(ii) Since $T_{FS}^\mu(A, B)$ remains unchanged after the replacement of A, B with A^c, B^c , this suggests that $T_{FS}^\mu(A^c, B^c) = T_{FS}^\mu(A, B)$. The fact, that $T_{FS}^\mu(A, B)$ is non-negative, can be established if we first inculcate the following **Lemma 3.1**.

Lemma 3.1 Define $N = \left(\frac{T_0 + E_0}{2}\right) \left(\sqrt{\frac{T_0^2 + E_0^2}{2}}\right)$, $A = \frac{T_0^2 + E_0^2}{2}$, $G = T_0 E_0$. There exists the

inequality: $4N \leq 3A + G$ with equality if $T_0^2 = \mu_A(x_i) = E_0^2 = \mu_B(x_i)$ (6)

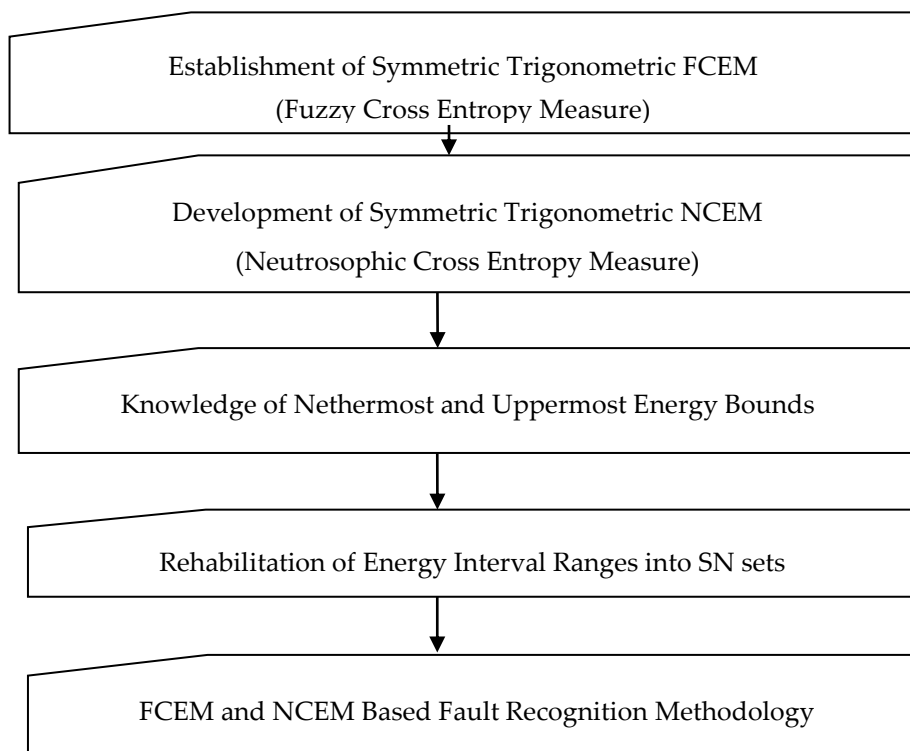


Fig. 1 A Step-wise Flow Chart of FCEM and NCEM Based urbine Fault Recognition Methodology

Proof. In our notations, we have

$$N = \left(\frac{T_0 + E_0}{2}\right) \left(\sqrt{\frac{T_0^2 + E_0^2}{2}}\right), A = \frac{T_0^2 + E_0^2}{2}, G = T_0 E_0.$$

The undergoing inequality (6) could be true if $2(T_0 + E_0) \left(\sqrt{\frac{T_0^2 + E_0^2}{2}}\right) \leq \frac{3}{2}(T_0^2 + E_0^2) + T_0 E_0$

$$\Leftrightarrow 8(T_0^2 + E_0^2 + 2T_0 E_0)(T_0^2 + E_0^2) \leq 9(T_0^2 + E_0^2)^2 + 4T_0^2 E_0^2 + 12(T_0^2 + E_0^2)T_0 E_0$$

$$\Leftrightarrow 8(T_0^2 + E_0^2)^2 + 16T_0 E_0 (T_0^2 + E_0^2) \leq 9(T_0^2 + E_0^2)^2 + 4T_0^2 E_0^2 + 12(T_0^2 + E_0^2)T_0 E_0$$

$$\Leftrightarrow (T_0^2 + E_0^2)^2 - 4(T_0^2 + E_0^2)T_0 E_0 + 4T_0^2 E_0^2 \geq 0$$

$$\Leftrightarrow (T_0^2 + E_0^2 - 2T_0 E_0)^2 \geq 0 \Leftrightarrow (T_0 - E_0)^4 \geq 0 \text{ which is obviously true.}$$

Thus, in view of the resulting **Lemma 3.1**, the inequality (6) can be rescheduled as

$$\frac{4N - G}{3} \leq A \Rightarrow \frac{4N - G}{3} + 1 \leq A + 1 \Rightarrow \frac{2(T_0 + E_0) \left(\sqrt{\frac{T_0^2 + E_0^2}{2}}\right) - T_0 E_0}{3} + 1 \leq \frac{T_0^2 + E_0^2}{2} + 1$$

$$\Rightarrow \frac{2+T_0^2+E_0^2}{3+2(T_0+E_0)\sqrt{\frac{T_0^2+E_0^2}{2}-T_0E_0}} \geq \frac{2}{3} \quad \dots (7)$$

Since tangent function exhibits the monotonicity property over $[0,1]$, the resulting inequality (7)

can be rescheduled as

$$(2+T_0^2+E_0^2)\tan \frac{2}{3} \geq (2+T_0^2+E_0^2)\tan \frac{2}{3} \dots (8)$$

With the replacement of $\mu_A(x_i)$ with $1-\mu_A(x_i)$ and of $\mu_B(x_i)$ with $1-\mu_B(x_i)$ into (8), we observe that

T_0^2 changes to $T_1^2 = 1-T_0^2$; $E_0^2 \rightarrow E_1^2 = 1-E_0^2$; $T_0+E_0 \rightarrow T_1+E_1$; $T_0E_0 \rightarrow T_1E_1$. Thus, (8) yields

$$(4-T_0^2-E_0^2)\tan \frac{2}{3} \geq (4-T_0^2-E_0^2)\tan \frac{2}{3} \dots (9)$$

We can simply add the resulting inequalities (8, 9) and then take the summation over $i=1$ to n to yield $T_{FS}^\mu(A,B) \geq 0$ as desired. Moreover, when $\mu_A(x_i) = \mu_B(x_i)$, then

$T_0 = E_0, T_1 = E_1, 1-T_0^2 = T_1^2, \sqrt{1-T_0^2} = T_1$. Also,

$$T_{FS}^\mu(A,A) = \sum_{i=1}^n \left[-6 \tan\left(\frac{2}{3}\right) + (2+2T_0^2)\tan\left(\frac{2+2T_0^2}{3+3T_0^2}\right) + (4-2T_0^2)\tan\left(\frac{4-2T_0^2}{6-3T_0^2}\right) \right] = 0 \quad \dots (10)$$

The equality (10) justifies that $T_{FS}^\mu(A,B) = 0$ whenever $\mu_A(x_i) = \mu_B(x_i)$ as desired.

After the establishment of proposed fuzzy cross entropy measure $T_{FS}^\mu(A,B)$, the next Theorem 3.3 argues the urgent situation under which it will admits its extreme values.

Theorem 3.3 If $n \in N$ is the cardinality of X , then

$$0 \leq T_{FS}^\mu(A,B) \leq 6 \left(\tan \frac{3\sqrt{2}}{3\sqrt{2}+2} - \tan \frac{2}{3} \right) n. \quad \dots (11)$$

Proof. If we replace the fuzzy set B with A^c , we observe that E_0^2 changes to $1-T_0^2$; $E_1 \rightarrow T_0, E_0 \rightarrow T_1, T_0T_1 \rightarrow T_2$.

Thus, after the replacement of $\mu_B(x_i)$ with $1-\mu_A(x_i)$, the undergoing equality measure (5) yields

$$T_{FS}^\mu(A,A^c) = \sum_{i=1}^n \left[6 \tan \frac{3\sqrt{2}}{3\sqrt{2}+2} - 6 \tan\left(\frac{2}{3}\right) - 6 \left(\tan\left(\frac{3\sqrt{2}}{3\sqrt{2}+2}\right) - \tan\left(\frac{3\sqrt{2}}{3\sqrt{2}+2(T_0+T_1)-\sqrt{2}T_2}\right) \right) \right]$$

$$= 6\text{Max.}T_F(A) - 6T_F(A) \quad \dots (12)$$

Because $T_F(A)$ is non-negative (**Theorem 3.1**), this motivates (12) to yield

$$T_F(A) = \text{Max.}T_F(A) - \frac{1}{6}T_{FS}^\mu(A, A^c) \geq 0 \Rightarrow 0 \leq T_{FS}^\mu(A, A^c) \leq 6 \left(\tan \frac{3\sqrt{2}}{3\sqrt{2}+2} - \tan \frac{2}{3} \right) n \quad \dots (13)$$

With the establishment of resulting inequality (13), it is informative to know that $T_{FS}^\mu(A, A^c)$ is finite for a fixed n. This justifies the finiteness of our proposed symmetric trigonometric FCEM (fuzzy cross entropy measure) which ranges as $0 \leq T_{FS}^\mu(A, B) \leq 6 \left(\tan \frac{3\sqrt{2}}{3\sqrt{2}+2} - \tan \frac{2}{3} \right) n$. Thus,

$$\text{Max.}T_{FS}^\mu(A, B) = \left(6 \tan \frac{3\sqrt{2}}{3\sqrt{2}+2} - \frac{2}{3} \right) n$$

which clarifies that this maximum value does not depend upon its truth membership degree, but completely depends upon the cardinality of X. Also, the surface plot of $T_{FS}^\mu(A, B)$, represented by **Fig 3(a, b)**, justifies the fact that this measure, because of its convexity, admits its $\text{Min.}T_{FS}^\mu(A, B) = 0$. Also, it is evident that $T_{FS}^\mu(A, B)$ gets increased as soon

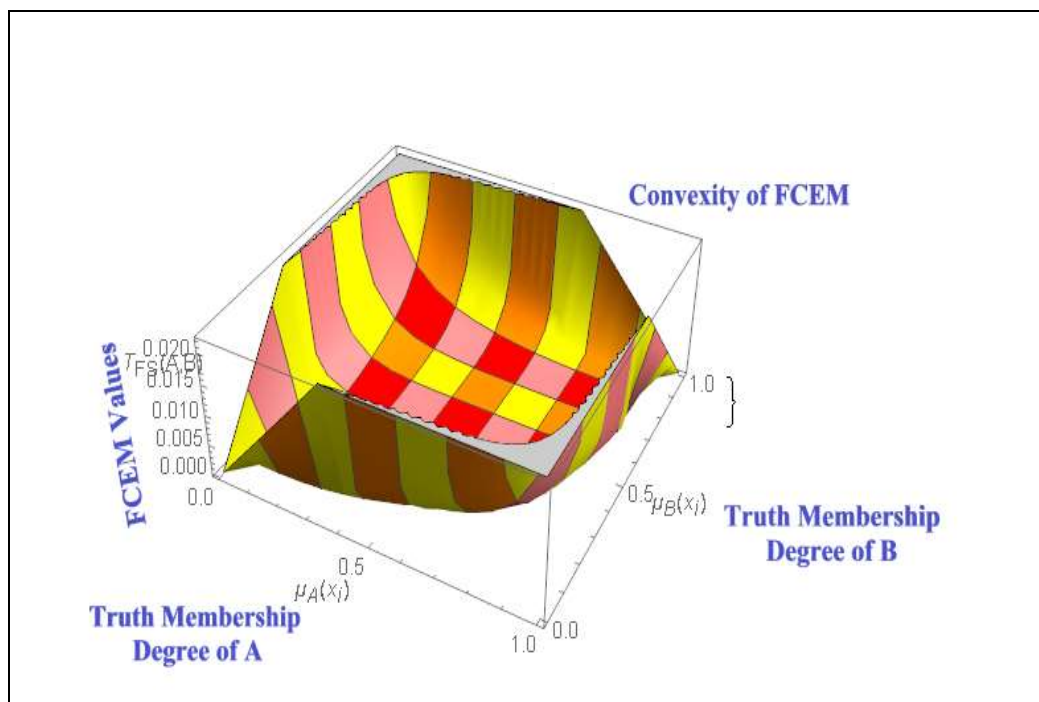
$$\text{as } |A - B| \text{ increases, attains } \text{Max.}T_{FS}^\mu(A, B) = 6 \left(\tan \frac{3\sqrt{2}}{3\sqrt{2}+2} - \tan \frac{2}{3} \right) n.$$

The establishment of FCEM $T_{FS}^\mu(A, B)$, resulted from **Theorem 3.2** in the overhead discussion, will lead to develop the proposed NCEM (represented by $T_{NC}(A, B)$), the repercussions of which will be utilized to meet our goal of recognizing fault conditions of turbine.

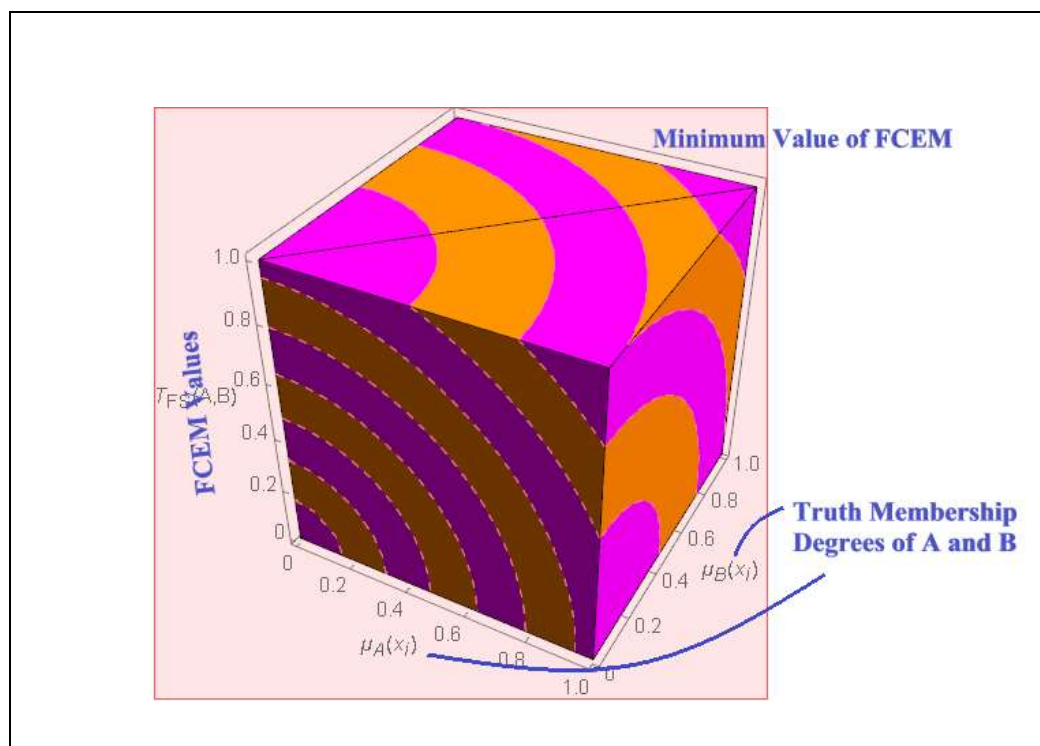
4. A Novel Symmetric Trigonometric NCEM (Neutrosophic Cross Entropy Measure)

In the resulting **Theorem 3.2**, the entity $T_{FS}^\mu(A, B)$ represents the amount of fuzziness which arises due to true membership degree for symmetric discrimination of fuzzy set A against B. Similarly, if we set $I_0 = \sqrt{i_A(x_i)}, I_1 = \sqrt{1-i_A(x_i)}, J_0 = \sqrt{i_B(x_i)}, J_1 = \sqrt{1-i_B(x_i)}$, then the amount of fuzziness which arises due to indeterminancy membership degree of A against B is established as

$$\begin{aligned}
 & T_{FS}^i(A, B) \\
 &= \sum_{i=1}^n \left[-6 \tan\left(\frac{2}{3}\right) \right. \\
 &\quad \left. + (2 + I_0^2 + J_0^2) \tan\left(\frac{2 + I_0^2 + J_0^2}{3 + 2(I_0 + J_0) \sqrt{\frac{I_0^2 + J_0^2}{2}} - I_0 J_0} \right) + (4 - I_0^2 - J_0^2) \tan\left(\frac{4 - I_0^2 - J_0^2}{3 + 2(I_1 + J_1) \sqrt{\frac{2 - I_0^2 - J_0^2}{2}} - I_1 J_1} \right) \right] \\
 & \dots (14)
 \end{aligned}$$



(a)



(b)

Fig 3 (a) Convexity and (b) Minimum Value of the proposed of FCEM $T_{FS}^{\mu}(A, B)$

Again, we set $F_0 = \sqrt{f_A(x_i)}, F_1 = \sqrt{1-f_A(x_i)}, H_0 = \sqrt{f_B(x_i)}, H_1 = \sqrt{1-f_B(x_i)}$, then the amount of fuzziness which arises due to falsity membership degree for symmetric discrimination of A against B can also be established as

$$\begin{aligned}
 & T_{FS}^f(A, B) \\
 &= \sum_{i=1}^n \left[-6 \tan\left(\frac{2}{3}\right) + (2 + F_0^2 + H_0^2) \tan\left(\frac{2 + F_0^2 + H_0^2}{3 + 2(F_0 + H_0)\sqrt{\frac{F_0^2 + H_0^2}{2}} - F_0 H_0}\right) + (4 - F_0^2 - H_0^2) \tan\left(\frac{4 - F_0^2 - H_0^2}{3 + 2(F_1 + H_1)\sqrt{\frac{2 - F_0^2 - H_0^2}{2}} - F_1 H_1}\right) \right] \dots (15)
 \end{aligned}$$

Def.4.1 Let A and B are any two SN sets in $X = (x_1, x_2, \dots, x_n)$. The desired NCEM (symmetric trigonometric neutrosophic cross entropy measure of SN sets can be constructed by simply adding (12), (14) and (15) as below.

$$T_{NC}(A, B) = T_{FS}^{\mu}(A, B) + T_{FS}^i(A, B) + T_{FS}^f(A, B) \dots (16)$$

Following same procedure as deployed in **Theorem 3.3**, readers can easily establish that if A and B are any SN sets with same cardinality n , then there exists the inequality:

$$0 \leq T_{NC}(A,B) \leq 18 \left(\tan \frac{3\sqrt{2}}{3\sqrt{2}+2} - \tan \frac{2}{3} \right) n.$$

We shall now authenticate the applicability of our newly discovered NCEM $T_{NC}(A,B)$ by recognizing the optimal fault condition of some huge steam turbine generator as follows.

6. FCEM and NCEM Based Fault Recognition Methodology

To achieve the desired goal, we shall, equally well, establish a neutrosophic cross entropy-based methodology which has the necessary capability of identifying various fault conditions of some turbine. A schematic flow chart explaining our fault recognition methodology has been provided in Fig. 1 and discussed as below.

Step:-1 Construction of Energy Interval Ranges

The applicability of the underlying methodology is exemplified by taking into consideration the illustration [12]. Suppose the ten familiar fault conditions experienced by some huge steam turbine generator set is represented by $B_K = (B_1, B_2, B_3, \dots, B_{10})$ where the fault condition “Unbalance” is abbreviated as B_1 . Similarly, the conditions B_2, B_3, \dots, B_{10} have been provided in [2,3]. Also, the nine frequency intervals $C_1 = [0.01, 0.3 f], C_2 = [0.4, 0.49 f], \dots, C_9 = \text{higher frequency} > 5 f$, of frequency spectrum, resulted from vibration signals of turbine, are available in [2,3].

Let $\mu_{B_K}(x_i)$ (lower bound) and $U_{B_K}(x_i)$ (upper bound) represent the amount of fuzziness resulted from the truth membership degree of K^{th} fault condition at i^{th} range of frequency spectrum. Then

$$B_K = (\langle x_1, [\mu_{B_K}(x_1), U_{B_K}(x_1)] \rangle, \langle x_2, [\mu_{B_K}(x_2), U_{B_K}(x_2)] \rangle, \dots, \langle x_9, [\mu_{B_K}(x_9), U_{B_K}(x_9)] \rangle); K = 1, 2, \dots, 10. \dots (17)$$

Generally, the acquitted vibration data may be non-commensurate and conflicting, it becomes essential for us to transform the energy interval ranges (17) into the form of SN sets. This conversion, however may be problematic, but can be done as follows.

Step:-2 Transformation of Interval Ranges (energy) by the Form of Neutrosophic Sets

The amount of fuzziness based on falsity membership degree of K^{th} familiar fault condition at i^{th} range of frequency spectrum is denoted by $f_{B_K}(x_i)$ where $f_{B_K}(x_i) = 1 - U_{B_K}(x_i)$. Similarly, the

amount of fuzziness based on indeterminacy membership degree of K^{th} familiar fault condition at i^{th} range of frequency spectrum is denoted by $i_{B_k}(x_i)$ where $i_{B_k}(x_i) = 1 - f_{B_k}(x_i) - U_{B_k}(x_i)$. We have restricted the value of $i_{B_k}(x_i)$ to 0.001 in case it if returns any other value less than or equal to 0.001. Then, the interval ranges (energy), represented by (17), for each B_k can be transformed into the forms of SN sets is described below.

$$B_K = \left(\left(\langle x_1, [\mu_{B_k}(x_1), i_{B_k}(x_1), f_{B_k}(x_1)] \rangle \right), \left(\langle x_2, [\mu_{B_k}(x_2), i_{B_k}(x_2), f_{B_k}(x_2)] \rangle \right), \right. \\ \left. \left(\langle x_3, [\mu_{B_k}(x_3), i_{B_k}(x_3), f_{B_k}(x_3)] \rangle \right), \dots, \left(\langle x_9, [\mu_{B_k}(x_9), i_{B_k}(x_9), f_{B_k}(x_9)] \rangle \right) \right); K = 1, 2, \dots, 10 \quad \dots (18)$$

Also, the unfamiliar fault conditions, represented by F_{T_j} , can also be transformed into the forms of SN sets as below:

$$F_{T_j} = \left(\left(\langle x_1, [\mu_{F_{T_j}}(x_1), i_{F_{T_j}}(x_1), f_{F_{T_j}}(x_1)] \rangle \right), \left(\langle x_2, [\mu_{F_{T_j}}(x_2), i_{F_{T_j}}(x_2), f_{F_{T_j}}(x_2)] \rangle \right), \right. \\ \left. \left(\langle x_3, [\mu_{F_{T_j}}(x_3), i_{F_{T_j}}(x_3), f_{F_{T_j}}(x_3)] \rangle \right), \dots, \left(\langle x_9, [\mu_{F_{T_j}}(x_9), i_{F_{T_j}}(x_9), f_{F_{T_j}}(x_9)] \rangle \right) \right) \quad \dots (19)$$

Step: -3 Computation of FCEM and NCEM Values between familiar and unfamiliar fault conditions

The cross-entropy values $T_{NC}(B_K, F_{T_j}), T_{FS}^\mu(B_K, F_{T_j})$ between each B_K and F_{T_j} can be evaluated as follows. Replacement of introduced notations T_0, F_0, H_0, \dots , etc., with their original values and then taking $i = 1, 2, \dots, 9$ into (5,16) yields

$$T_{FS}^\mu(B_K, F_{T_j}) \\ = \sum_{i=1}^9 \left[\begin{aligned} & -6 \tan \frac{2}{3} + (2 + \mu_{B_k}(x_i) + \mu_{F_{T_j}}(x_i)) \tan \left(\frac{2 + \mu_{B_k}(x_i) + \mu_{F_{T_j}}(x_i)}{3 + 2 \left(\sqrt{\mu_{B_k}(x_i)} + \sqrt{\mu_{F_{T_j}}(x_i)} \right) \left(\frac{\sqrt{\mu_{B_k}(x_i)} + \mu_{F_{T_j}}(x_i)}{2} \right) - \sqrt{\mu_{B_k}(x_i)} \mu_{F_{T_j}}(x_i)} \right) \\ & - (4 - \mu_{B_k}(x_i) - \mu_{F_{T_j}}(x_i)) \tan \left(\frac{4 - \mu_{B_k}(x_i) - \mu_{F_{T_j}}(x_i)}{3 + 2 \left(\sqrt{1 - \mu_{B_k}(x_i)} + \sqrt{1 - \mu_{F_{T_j}}(x_i)} \right) \left(\frac{\sqrt{2 - \mu_{B_k}(x_i)} - \mu_{F_{T_j}}(x_i)}{2} \right) - \sqrt{(1 - \mu_{B_k}(x_i))(1 - \mu_{F_{T_j}}(x_i))}} \right) \end{aligned} \right] \quad \dots (20)$$

$$\begin{aligned}
 & T_{NC}(B_K, F_{T_j}) \\
 &= \sum_{i=1}^9 \left[\begin{aligned} & -6 \tan \frac{2}{3} + (2 + \mu_{B_K}(x_i) + \mu_{F_{T_j}}(x_i)) \tan \left(\frac{2 + \mu_{B_K}(x_i) + \mu_{F_{T_j}}(x_i)}{3 + 2 \left(\sqrt{\mu_{B_K}(x_i)} + \sqrt{\mu_{F_{T_j}}(x_i)} \right) \left(\frac{\sqrt{\mu_{B_K}(x_i) + \mu_{F_{T_j}}(x_i)}}{2} \right) - \sqrt{\mu_{B_K}(x_i) \mu_{F_{T_j}}(x_i)}} \right)} \\ & - (4 - \mu_{B_K}(x_i) - \mu_{F_{T_j}}(x_i)) \tan \left(\frac{4 - \mu_{B_K}(x_i) - \mu_{F_{T_j}}(x_i)}{3 + 2 \left(\sqrt{1 - \mu_{B_K}(x_i)} + \sqrt{1 - \mu_{F_{T_j}}(x_i)} \right) \left(\frac{\sqrt{2 - \mu_{B_K}(x_i) - \mu_{F_{T_j}}(x_i)}}{2} \right) - \sqrt{(1 - \mu_{B_K}(x_i))(1 - \mu_{F_{T_j}}(x_i))}} \right)} \end{aligned} \right] \\
 &+ \sum_{i=1}^9 \left[\begin{aligned} & -6 \tan \frac{2}{3} + (2 + i_{B_K}(x_i) + i_{F_{T_j}}(x_i)) \tan \left(\frac{2 + i_{B_K}(x_i) + i_{F_{T_j}}(x_i)}{3 + 2 \left(\sqrt{i_{B_K}(x_i)} + \sqrt{i_{F_{T_j}}(x_i)} \right) \left(\frac{\sqrt{i_{B_K}(x_i) + i_{F_{T_j}}(x_i)}}{2} \right) - \sqrt{i_{B_K}(x_i) i_{F_{T_j}}(x_i)}} \right)} \\ & - (4 - i_{B_K}(x_i) - i_{F_{T_j}}(x_i)) \tan \left(\frac{4 - i_{B_K}(x_i) - i_{F_{T_j}}(x_i)}{3 + 2 \left(\sqrt{1 - i_{B_K}(x_i)} + \sqrt{1 - i_{F_{T_j}}(x_i)} \right) \left(\frac{\sqrt{2 - i_{B_K}(x_i) - i_{F_{T_j}}(x_i)}}{2} \right) - \sqrt{(1 - i_{B_K}(x_i))(1 - i_{F_{T_j}}(x_i))}} \right)} \end{aligned} \right] \\
 &+ \sum_{i=1}^9 \left[\begin{aligned} & -6 \tan \frac{2}{3} + (2 + f_{B_K}(x_i) + f_{F_{T_j}}(x_i)) \tan \left(\frac{2 + f_{B_K}(x_i) + f_{F_{T_j}}(x_i)}{3 + 2 \left(\sqrt{f_{B_K}(x_i)} + \sqrt{f_{F_{T_j}}(x_i)} \right) \left(\frac{\sqrt{f_{B_K}(x_i) + f_{F_{T_j}}(x_i)}}{2} \right) - \sqrt{f_{B_K}(x_i) f_{F_{T_j}}(x_i)}} \right)} \\ & - (4 - f_{B_K}(x_i) - f_{F_{T_j}}(x_i)) \tan \left(\frac{4 - f_{B_K}(x_i) - f_{F_{T_j}}(x_i)}{3 + 2 \left(\sqrt{1 - f_{B_K}(x_i)} + \sqrt{1 - f_{F_{T_j}}(x_i)} \right) \left(\frac{\sqrt{2 - f_{B_K}(x_i) - f_{F_{T_j}}(x_i)}}{2} \right) - \sqrt{(1 - f_{B_K}(x_i))(1 - f_{F_{T_j}}(x_i))}} \right)} \end{aligned} \right] \\
 & \dots (21)
 \end{aligned}$$

Step: -4 Identification of Turbine Faults

The Smallest value of $T_{NC}(B_K, F_{T_j}); T_{FS}^\mu(B_K, F_{T_j})$ indicate that the familiar fault condition B_K is closer to the unfamiliar fault condition F_{T_j} . In other words, a typical selection of turbine fault will be designated as optimal fault type selection owing to the smallest NCEM $T_{NC}(B_K, F_{T_j})$ or FCEM $T_{FS}^\mu(B_K, F_{T_j})$ value.

7. APPLICATION TO FAULT DIAGNOSIS OF TURBINE

In order to validate the applicability of FCEM and NCEM based fault recognition methodology, the energy interval ranges for each familiar fault condition at various ranges of frequency spectrum is provided in **Table 1**.

Table 1. The Nethermost and Uppermost Energy Bounds of Each B_k at Nine Ranges of frequency Spectrum

B_k	C_1	C_2	C_3	C_4	C_5	C_6	C_7	C_8	C_9
B_1	[0.00,0.00]	[0.00,0.00]	[0.00,0.00]	[0.00,0.00]	[0.85,1.00]	[0.04,0.06]	[0.04,0.07]	[0.00,0.00]	[0.00,0.00]
B_2	[0.00,0.00]	[0.03,0.31]	[0.90,0.12]	[0.55,0.70]	[0.00,0.00]	[0.00,0.00]	[0.00,0.00]	[0.00,0.00]	[0.08,0.13]
B_3	[0.00,0.00]	[0.00,0.00]	[0.00,0.00]	[0.00,0.00]	[0.30,0.58]	[0.40,0.62]	[0.08,0.13]	[0.00,0.00]	[0.00,0.00]
B_4	[0.09,0.11]	[0.78,0.82]	[0.00,0.00]	[0.08,0.11]	[0.00,0.00]	[0.00,0.00]	[0.00,0.00]	[0.00,0.00]	[0.00,1.00]
B_5	[0.09,0.12]	[0.09,0.11]	[0.08,0.12]	[0.09,0.12]	[0.18,0.21]	[0.08,0.13]	[0.08,0.13]	[0.08,0.22]	[0.08,0.12]
B_6	[0.00,0.00]	[0.00,0.00]	[0.00,0.00]	[0.00,0.00]	[0.18,0.22]	[0.12,0.17]	[0.37,0.45]	[0.00,0.00]	[0.22,0.28]
B_7	[0.00,0.00]	[0.00,0.00]	[0.08,0.12]	[0.86,0.93]	[0.00,0.00]	[0.00,0.00]	[0.00,0.00]	[0.00,0.00]	[0.00,0.00]
B_8	[0.00,0.00]	[0.27,0.32]	[0.08,0.12]	[0.54,0.62]	[0.00,0.00]	[0.00,0.00]	[0.00,0.00]	[0.00,0.00]	[0.00,0.00]
B_9	[0.85,0.93]	[0.00,0.00]	[0.00,0.00]	[0.00,0.00]	[0.00,0.00]	[0.00,0.00]	[0.00,0.00]	[0.08,0.12]	[0.00,0.00]
B_{10}	[0.00,0.00]	[0.00,0.00]	[0.00,0.00]	[0.00,0.00]	[0.00,0.00]	[0.77,0.83]	[0.19,0.30]	[0.00,0.00]	[0.00,0.00]

Table 2. Transforming B_k into the forms of Single valued neutrosophic (SN) Sets

C_1	C_2	C_3	C_4	C_5	C_6	C_7	C_8	C_9
[0.00,0.01,1.00]	[0.00,0.01,1.00]	[0.00,0.01,1.00]	[0.00,0.01,1.00]	[0.85,0.15,0.00]	[0.04,0.02,0.94]	[0.04,0.03,0.93]	[0.00,0.01,1.00]	[0.00,0.01,1.00]
[0.00,0.01,1.00]	[0.03,0.01,0.69]	[0.90,0.03,0.88]	[0.55,0.15,0.30]	[0.00,0.01,1.00]	[0.00,0.01,1.00]	[0.00,0.01,1.00]	[0.00,0.01,1.00]	[0.08,0.05,0.87]
[0.00,0.01,1.00]	[0.00,0.01,1.00]	[0.00,0.01,1.00]	[0.00,0.01,1.00]	[0.30,0.28,0.42]	[0.40,0.22,0.38]	[0.08,0.05,0.87]	[0.00,0.01,1.00]	[0.00,0.01,1.00]
[0.09,0.02,0.89]	[0.78,0.04,0.18]	[0.00,0.01,1.00]	[0.08,0.03,0.89]	[0.00,0.01,1.00]	[0.00,0.01,1.00]	[0.00,0.01,1.00]	[0.00,0.01,1.00]	[0.00,0.01,1.00]
[0.09,0.03,0.88]	[0.09,0.02,0.89]	[0.08,0.04,0.88]	[0.09,0.03,0.88]	[0.18,0.03,0.79]	[0.08,0.05,0.87]	[0.08,0.05,0.87]	[0.08,0.04,0.88]	[0.08,0.04,0.88]
[0.00,0.01,1.00]	[0.00,0.01,1.00]	[0.00,0.01,1.00]	[0.00,0.01,1.00]	[0.18,0.04,0.78]	[0.12,0.05,0.83]	[0.37,0.08,0.55]	[0.00,0.01,1.00]	[0.22,0.06,0.72]
[0.00,0.01,1.00]	[0.00,0.01,1.00]	[0.08,0.04,0.88]	[0.86,0.07,0.07]	[0.00,0.01,1.00]	[0.00,0.01,1.00]	[0.00,0.01,1.00]	[0.00,0.01,1.00]	[0.00,0.01,1.00]
[0.00,0.01,1.00]	[0.27,0.05,0.68]	[0.08,0.04,0.88]	[0.54,0.08,0.38]	[0.00,0.01,1.00]	[0.00,0.01,1.00]	[0.00,0.01,1.00]	[0.00,0.01,1.00]	[0.00,0.01,1.00]
[0.85,0.08,0.07]	[0.00,0.01,1.00]	[0.00,0.01,1.00]	[0.00,0.01,1.00]	[0.00,0.01,1.00]	[0.00,0.01,1.00]	[0.00,0.01,1.00]	[0.08,0.04,0.88]	[0.00,0.01,1.00]
[0.00,0.01,1.00]	[0.00,0.01,1.00]	[0.00,0.01,1.00]	[0.00,0.01,1.00]	[0.00,0.01,1.00]	[0.77,0.06,0.17]	[0.19,0.04,0.77]	[0.00,0.01,1.00]	[0.00,0.01,1.00]

Step:-2 The nethermost (lowest) and uppermost (highest) energy bounds of each real fault conditions (B_k) have been extracted and thereafter rehabilitated into the forms of SN sets as

shown in **Table 2**. The fault testing samples F_{T_j} ($J = 1, 2$) in this study can also be transformed into the forms of SN sets as follows.

$$F_{T_1} = \left\langle \begin{matrix} [0.000, 0.010, 1.000], [0.000, 0.010, 1.000], [0.100, 0.010, 0.900], [0.000, 0.010, 1.000], \\ [0.000, 0.010, 1.000], [0.000, 0.010, 1.000], [0.000, 0.010, 1.000], [0.000, 0.010, 1.000], \\ [0.000, 0.010, 1.000] \end{matrix} \right\rangle \quad \dots \quad (22)$$

$$F_{T_2} = \left\langle \begin{matrix} [0.390, 0.010, 0.610], [0.070, 0.010, 0.930], [0.000, 0.010, 1.000], [0.060, 0.010, 0.940], \\ [0.000, 0.010, 1.000], [0.130, 0.010, 0.870], [0.000, 0.010, 1.000], [0.000, 0.010, 1.000], \\ [0.350, 0.010, 0.650] \end{matrix} \right\rangle \quad \dots \quad (23)$$

Step:- 3 The FCEM $T_{FS}^\mu(B_K, F_{T_j})$ and NCEM $T_{NC}(B_K, F_{T_j})$ values between each B_K (provided in **Table 2**) and F_{T_j} (represented by (22,23)) can be computed employing the resulting equations (20,21). The fault diagnosis order obtained through the proposed FCEM and NCEM as well as by the existing cosine similarity measure [3] is represented in **Table 3**.

Diagnosis Result 1. The fuzzy as well as neutrosophic cross entropy values between each familiar fault condition B_K and the first testing sample F_{T_1} , as can be seen from **Table 3**, are

$$T_{FS}^\mu(B_1, F_{T_1}) = 0.1382, T_{FS}^\mu(B_2, F_{T_1}) = 0.0082, T_{FS}^\mu(B_3, F_{T_1}) = 0.1222; T_{FS}^\mu(B_4, F_{T_1}) = 0.0830, T_{FS}^\mu(B_5, F_{T_1}) = 0.0595,$$

$$T_{FS}^\mu(B_6, F_{T_1}) = 0.1289, T_{FS}^\mu(B_7, F_{T_1}) = 0.0000, T_{FS}^\mu(B_8, F_{T_1}) = 0.0184, T_{FS}^\mu(B_9, F_{T_1}) = 0.1382, T_{FS}^\mu(B_{10}, F_{T_1}) = 0.1368.$$

$$T_{NC}(B_1, F_{T_1}) = 0.3491, T_{NC}(B_2, F_{T_1}) = 0.0385, T_{NC}(B_3, F_{T_1}) = 0.2913; T_{NC}(B_4, F_{T_1}) = 0.1676, T_{NC}(B_5, F_{T_1}) = 0.1327,$$

$$T_{NC}(B_6, F_{T_1}) = 0.2737, T_{NC}(B_7, F_{T_1}) = 0.0006, T_{NC}(B_8, F_{T_1}) = 0.0401, T_{NC}(B_9, F_{T_1}) = 0.2931, T_{NC}(B_{10}, F_{T_1}) = 0.2824.$$

In view of Minimum Argument Principle, the minimum symmetric trigonometric FCEM and NCEM values are 0.0000 and 0.0006 respectively. Clearly, these values confirm that vibration fault in turbine occurs due to the defect in anti-thrust bearing (B_7), which is an optimal turbine fault selection, as it can also be experienced from **Fig. 4(a)**. The next smallest FCEM and NCEM values are 0.0082, 0.0184 and 0.0385, 0.0401 respectively which correspond to the fault types B_2 and B_8 . This indicates that there is a high possibility of pneumatic force couple and surge faults in the generator. The fault type B_5 (radial impact friction of rotor) has low possibility owing to the next smaller

FCEM and NCEM values (0.0595,0.1327). Similarly, the fault types $B_4, B_6, B_{10}, B_3, B_9$ and B_1 have very low possibility owing to their smaller FCEM and NCEM entropy values.

Table 3. Fault Recognition of Turbine employing (a) FCEM (b) NCEM and (b) Existing Cosine Similarity Measure [3]

Description	Measure Values	Recognized Fault Condition	Actual Fault Condition
FCEM	FCEM Values		
$T_{FS}^{\mu}(B_K, F_{T_1})$	0.1382 0.0082 0.1222 0.0830 0.0595	Antithrust Bearing	Antithrust Bearing
	0.1289 0.0000 0.0184 0.13821 0.1368		
$T_{FS}^{\mu}(B_K, F_{T_2})$	0.1170 0.0445 0.0787 0.0424 0.0282	Radial Impact Friction	Radial Impact Friction
	0.0670 0.0818 0.0651 0.0448 0.0720		
NCEM	NCEM Values		
$T_{NC}(B_K, F_{T_1})$	0.3491 0.0385 0.2913 0.1676 0.1327	Antithrust Bearing	Antithrust Bearing
	0.2737 0.0006 0.0401 0.2931 0.2824		
$T_{NC}(B_K, F_{T_2})$	0.3053 0.0901 0.1916 0.0867 0.0584	Radial Impact Friction	Radial Impact Friction
	0.1428 0.1679 0.1284 0.0967 0.1493		
Cosine	Cosine Similarity Measure Value []		
$C_{VS}(B_K, F_{T_1})$	0.7891 0.9799 0.8282 0.8236 0.9057	Antithrust Bearing	Antithrust Bearing
	0.8714 0.9995 0.9774 0.7974 0.8099		
$C_{VS}(B_K, F_{T_2})$	0.8563 0.9128 0.9066 0.8953 0.9738	Radial Impact Friction	Radial Impact Friction
	0.9567 0.8720 0.9201 0.9403 0.8968		

Thus, the optimal fault recognition order is

$$B_7 \succ B_2 \succ B_8 \succ B_5 \succ B_4 \succ B_3 \succ B_6 \succ B_{10} \succ B_1 \succ B_9 \text{ (Obtained from FCEM)}$$

$$B_7 \succ B_2 \succ B_8 \succ B_5 \succ B_4 \succ B_6 \succ B_{10} \succ B_3 \succ B_9 \succ B_1 \text{ (Obtained from NCEM)}$$

Diagnosis Result 2. The FCEM and NCEM values between second real testing sample F_{T_2} and B_K are

$$T_{FS}^{\mu}(B_1, F_{T_2}) = 0.1170, T_{FS}^{\mu}(B_2, F_{T_2}) = 0.0445, T_{FS}^{\mu}(B_3, F_{T_2}) = 0.0787, T_{FS}^{\mu}(B_4, F_{T_2}) = 0.0424, T_{FS}^{\mu}(B_5, F_{T_2}) = 0.0282,$$

$$T_{FS}^{\mu}(B_6, F_{T_2}) = 0.0670, T_{FS}^{\mu}(B_7, F_{T_2}) = 0.0818, T_{FS}^{\mu}(B_8, F_{T_2}) = 0.0651, T_{FS}^{\mu}(B_9, F_{T_2}) = 0.0448, T_{FS}^{\mu}(B_{10}, F_{T_2}) = 0.0720.$$

$$T_{NC}(B_1, F_{T_2}) = 0.3053, T_{NC}(B_2, F_{T_2}) = 0.0901, T_{NC}(B_3, F_{T_2}) = 0.1916, T_{NC}(B_4, F_{T_2}) = 0.0867, T_{NC}(B_5, F_{T_2}) = 0.0584,$$

$$T_{NC}(B_6, F_{T_2}) = 0.1428, T_{NC}(B_7, F_{T_2}) = 0.1679, T_{NC}(B_8, F_{T_2}) = 0.1284, T_{NC}(B_9, F_{T_2}) = 0.0967, T_{NC}(B_{10}, F_{T_2}) = 0.1493.$$

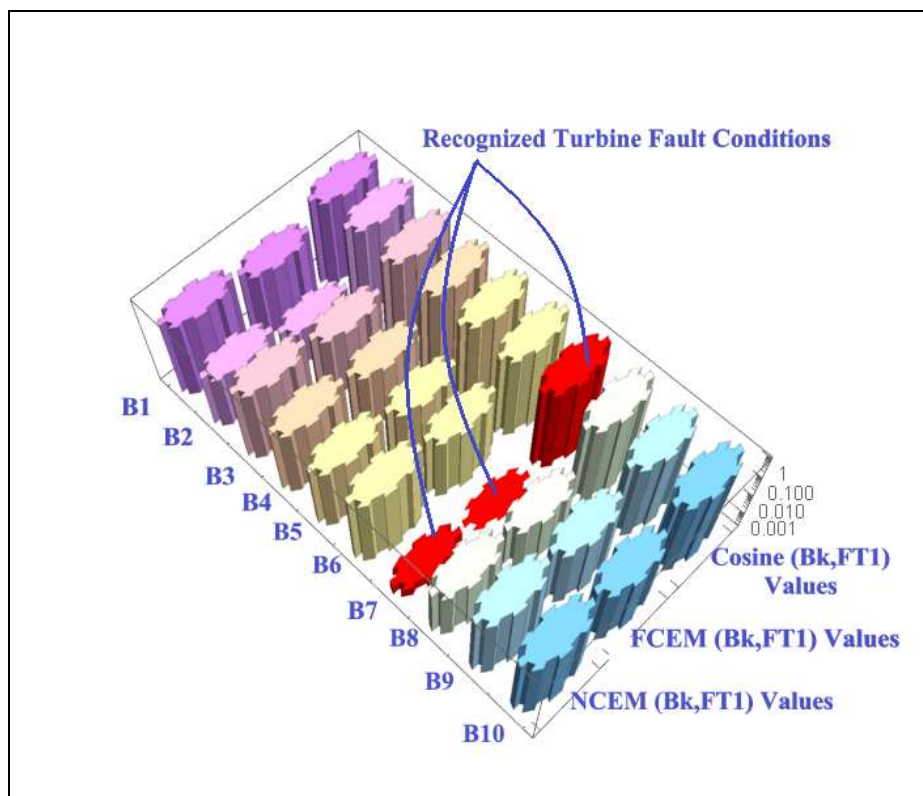


Fig.4(a) Recognized Optimal Fault Condition Employing Proposed Fuzzy, Neutrosophic Cross Entropy and Existing Cosine Similarity Measures [3]

In this case, the minimum symmetric trigonometric FCEM and NCEM values are 0.0282 and 0.0584 respectively. Clearly, these values confirm that vibration fault in turbine occurs due to the defect in radial impact friction of the rotor (B_5), which is an optimal turbine fault selection, as it can also be

experienced from **Fig. 4(b)**. The next smallest FCEM and NCEM values are 0.0424,0.0445 and 0.0584,0.0901 respectively which correspond to the fault types B_4 and B_2 . This indicates that there is a high possibility of pneumatic force couple and oil membrane oscillation. The fault type B_9 (looseness of bearing block) has low possibility owing to its smaller FCEM and NCEM values (0.0448,0.0967). Similarly, the fault types $B_8, B_6, B_{10}, B_7, B_3$ and B_1 have very low possibility owing to their smaller cross entropy values. Thus, the optimal fault recognition order is $B_5 > B_4 > B_2 > B_9 > B_8 > B_6 > B_{10} > B_7 > B_3 > B_1$.

Validity Test: In order to perform the validity of NCEM under validity criteria [11], we inter-change the degree of true and falsity membership of non-optimal (B_9) alternative and worse (B_1) alternatives. The new symmetric trigonometric FCEM and NCEM values can be recalculated employing (21) and are given below.

$$T_{NC}(B_1, F_{T_1}) = 1.4895, T_{NC}(B_2, F_{T_1}) = 0.0385, T_{NC}(B_3, F_{T_1}) = 0.2913, T_{NC}(B_4, F_{T_1}) = 0.1676, T_{NC}(B_5, F_{T_1}) = 0.1327,$$

$$T_{NC}(B_6, F_{T_1}) = 0.2737, T_{NC}(B_7, F_{T_1}) = 0.0006, T_{NC}(B_8, F_{T_1}) = 0.0401, T_{NC}(B_9, F_{T_1}) = 1.5678, T_{NC}(B_{10}, F_{T_1}) = 0.2824.$$

$$T_{NC}(B_1, F_{T_2})=1.1789, T_{NC}(B_2, F_{T_2})=0.0976, T_{NC}(B_3, F_{T_2})=1.1882, T_{NC}(B_4, F_{T_2})=0.0867, T_{NC}(B_5, F_{T_2})=0.0660,$$

$$T_{NC}(B_6, F_{T_2})=0.1428, T_{NC}(B_7, F_{T_2})=0.1754, T_{NC}(B_8, F_{T_2})=0.1360, T_{NC}(B_9, F_{T_2})=0.0967, T_{NC}(B_{10}, F_{T_2})=0.1493.$$

The results clearly indicate that the optimal fault selection does not change whenever we interchange the non-optimal and worse alternatives. This justifies that our proposed NCEM is capable of holding the best fault selection whenever worse and non-optimal are interchanged. However, the existing measures [2,3] are insufficient for holding the best fault selection. This indicates some ambiguity in the enduring fault recognition methods

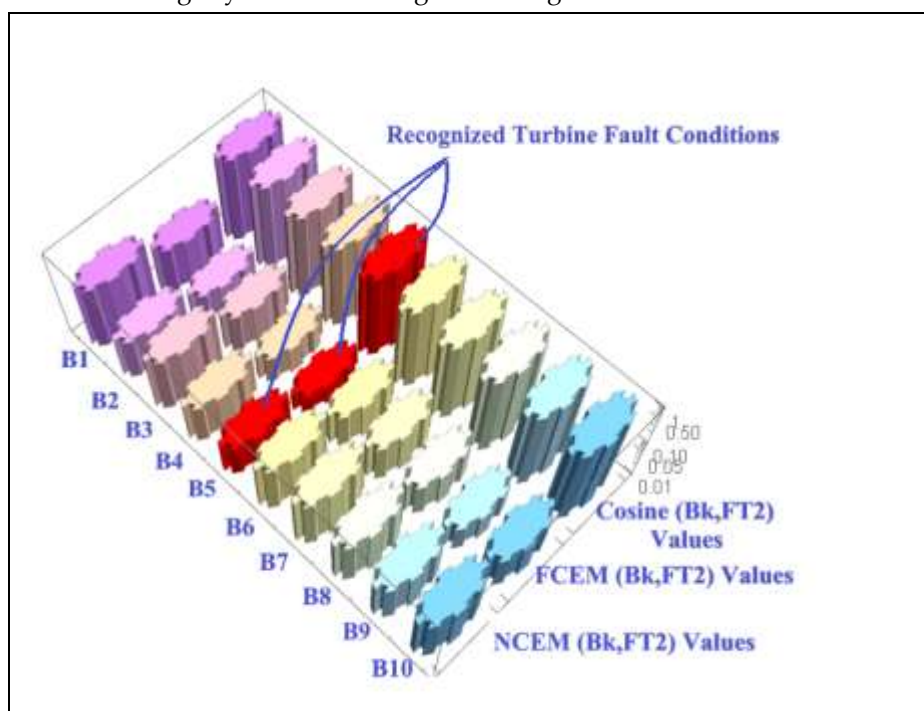


Fig.4(b) Recognized Optimal Fault Condition Employing Proposed Fuzzy, Neutrosophic Cross Entropy and Existing Cosine Similarity Measures

Table 4. Fault Recognition of Turbine employing (a) FCEM (b) NCEM and (b) Existing Cosine Similarity Measure [3] Under Sensitive Analysis

Description	Measure Values					Optimal, Worse Alternatives Under Sensitive Analysis	
	NCEM Values					Before	After
$T_{NC}(B_K, F_{T_1})$	0.3497	0.0391	0.2920	0.1682	0.1284	B_9, B_1	B_3, B_1
	0.2743	0.0012	0.0407	0.2887	0.2831		
$T_{NC}(B_K, F_{T_2})$	0.3059	0.0907	0.1922	0.0873	0.0541	B_3, B_1	B_3, B_1
	0.1434	0.1685	0.1290	0.0924	0.1499		

Sensitive Analysis In order to demonstrate the effectiveness of NCEM under sensitive analysis[11], we slightly change the value $(\langle x_8, [0.00, 0.01, 1.00] \rangle)$ of F_{T_1} to $(\langle x_8, [0.010, 0.010, 1.000] \rangle)$. Next, we again compute $T_{NC}(B_K, F_{T_j})(j=1,2)$ employing (21) and represent the results in ranking order of all ten knowledge of system faults is provided in Table 4. A The comparison of the results depicted in Table 3 and Table 4 indicate that the optimal and worse alternatives remain unchanged whenever there is a small change in the SN set $(\langle x_8, [0.00, 0.01, 1.00] \rangle)$. This clarifies that our symmetric trigonometric NCEM is an insensitive measure when subjected to a little change in the evaluation values. However, the enduring measures [2,3] have been found sensitive under this experiment.

Intuitive Analysis For the performance of FCEM, NCEM and existing measures [12] under intuitive analysis, we have assumed two fuzzy sets (F_1, F_2) and SN sets (T_1, T_2) as depicted in Table. In this experiment, we have fixed the value of F_2 as $[1.000]$, T_2 as $[1.000, 0.010, 0.000]$ meanwhile, the value of F_1, T_1 are increased gradually as presented in Table. The FCEM and NCEM values along with existing measure values [] are calculated using (20,21) and the results are presented Table 5. The tabulated results reveal that $T_{FS}^\mu(F_1, F_2); T_{NC}(T_1, T_2)$ values decrease whenever there is a slight increase in the values of F_1, T_1 . However, a constant or undefined trend was experienced while repeating this phenomenon with the enduring measures [2,3]. This justifies that fault information conveyed by proposed cross entropy measures are feasible and meaningful. Moreover, this also justifies the superiority and remarkability of proposed methodology over the enduring methods [2,3], under intuitive analysis.

Table 5. Intuitive analysis of (a) FCEM (b) NCEM (c) Existing Measures [2,3]

Gp. No.	Fuzzy Set		SN Set		FCEM	NCEM	Cosine[3]	Measure [3]
	F_1	F_2	T_1	T_2	Values	Values	Values	Values
1	0.000	1.000	[0.000,0.010,0.000]	[1.000,0.010,0.000]	0.1272	0.1272	0.0009	#NUM!
2	0.100	1.000	[0.100,0.010,0.000]	[1.000,0.010,0.000]	0.0672	0.0672	0.0905	1.1371
3	0.200	1.000	[0.200,0.010,0.000]	[1.000,0.010,0.000]	0.0544	0.0544	0.0908	1.1262
4	0.300	1.000	[0.300,0.010,0.000]	[1.000,0.010,0.000]	0.0457	0.0457	0.0909	1.1163

5	0.400	1.000	[0.400,0.010,0.000]	[1.000,0.010,0.000]	0.0384	0.0384	0.0909	1.1071
6	0.500	1.000	[0.500,0.010,0.000]	[1.000,0.010,0.000]	0.0316	0.0316	0.0909	1.0984
7	0.600	1.000	[0.600,0.010,0.000]	[1.000,0.010,0.000]	0.0251	0.0251	0.0909	1.0901
8	0.700	1.000	[0.700,0.010,0.000]	[1.000,0.010,0.000]	0.0188	0.0188	0.0909	1.0822
9	0.800	1.000	[0.800,0.010,0.000]	[1.000,0.010,0.000]	0.0124	0.0124	0.0909	1.0745
10	0.900	1.000	[0.900,0.010,0.000]	[1.000,0.010,0.000]	0.0062	0.0062	0.0909	1.0671
11	1.000	1.000	[1.000,0.010,0.000]	[1.000,0.010,0.000]	0.0000	0.0000	0.0909	#NUM!

Conclusion

This study has propounded the establishment of novel symmetric trigonometric fuzzy as well as single valued neutrosophic cross entropy measures (FCEM and NCEM). To overcome the shortcomings faced by non-fuzzy and asymmetrical cross entropy measures and to obtain meaningful fault information, the proposed symmetric FCEM and NCEM has the necessary capability for recognizing the optimal fault conditions such as antithrust bearing and radial impact of friction of rotor, of a huge steam turbine generator. The proposed variants of neutrosophic cross entropy measures are compatible for further mathematical treatments under sensitive and intuitive analysis because of their symmetric quintessence whereas the enduring measures exhibit inconsequential results indicating ambiguity in the evaluation information of fault features

Credit Authorship Contribution Statement:

C.P. Gandhi: Writing Original Draft, Methodology.

Declaration of Competing Interest The authors declare no conflict of interest.

References

- [1] He Ren, Wenyi Liu, Mengchen Shan, Xin Wang, Zhengfeng Wang (2021), "A novel wind turbine health condition monitoring method based on composite variational mode entropy and weighted distribution adaptation", Renewable Energy, Vol.168, pp.972-980.
- [2] Ye. Jun. (2009), "Fault diagnosis of turbine based on fuzzy cross entropy of vague sets", Experts Systems with Applications,36, p.8103-8106.
- [3] Shi.L.L., Ye. J., (2013), "Study on fault diagnosis of turbine using an improved cosine similarity measure of vague sets", Journal of Applied Sciences,13(10),p.1781-1786.
- [4] Shi.L.L.(2016), "Correlation coefficient of simplified neutrosophic sets for bearing fault diagnosis", Shock and Vibration,20(2), p.1-11.

- [5] Tian, Y., Wang, Z., Lu, C., 2019. Self-adaptive bearing fault diagnosis based on permutation entropy and manifold-based dynamic time warping. *Mechanical Systems and Signal Processing* 114, 658–673. <https://doi.org/10.1016/j.ymssp.2016.04.028>.
- [6] Camarena-Martinez, D., Valtierra-Rodriguez, M., Amezquita-Sanchez, J.P., Granados-Lieberman, D. Romero-Troncoso, R.J., Garcia-Perez, A., 2016. Shannon Entropy and -Means Method for Automatic Diagnosis of Broken Rotor Bars in Induction Motors Using Vibration Signals [WWW Document]. *Shock and Vibration*. <https://doi.org/10.1155/2016/4860309>.
- [7] Fu, L., He, Z.Y., Mai, R.K., Bo, Z.Q., 2009. Approximate entropy and its application to fault detection and identification in power swing, in: 2009 IEEE Power Energy Society General Meeting. Presented at the 2009 IEEE Power Energy Society General Meeting, pp. 1–8. <https://doi.org/10.1109/PES.2009.5275380>.
- [8] Zhao, L.-Y., Wang, L., Yan, R.-Q., 2015. Rolling Bearing Fault Diagnosis Based on Wavelet Packet Decomposition and Multi-Scale Permutation Entropy. *Entropy* 17, 6447–6461. <https://doi.org/10.3390/e17096447>
- [9] Zhang, X., Yan, Q., Yang, J., Zhao, J., Shen, Y., 2019. An assembly tightness detection method for bolt-jointed rotor with wavelet energy entropy. *Measurement* 136, 212–224. <https://doi.org/10.1016/j.measurement.2018.12.056>
- [10] Leite, G. de N.P., Araújo, A.M., Rosas, P.A.C., Stosic, T., Stosic, B., 2019. Entropy measures for early detection of bearing faults. *Physica A: Statistical Mechanics and its Applications* 514, 458–472. <https://doi.org/10.1016/j.physa.2018.09.052>.
- [11] Kumar, A., Gandhi, C.P., Zhou, Y., Tang, H., Xiang, J., 2020b. Fault diagnosis of rolling element bearing based on symmetric cross entropy of neutrosophic sets. *Measurement* 152, 107318. <https://doi.org/10.1016/j.measurement.2019.107318>
- [12] Kumar, A., Gandhi, C.P., Zhou, Y., Kumar, R., Xiang, J., 2020a. Variational mode decomposition based symmetric single valued neutrosophic cross entropy measure for the identification of bearing defects in a centrifugal pump. *Applied Acoustics* 165, 107294. <https://doi.org/10.1016/j.apacoust.2020.107294>
- [13] Kumar, A., Gandhi, C.P., Zhou, Y., Tang, H., Xiang, J., 2020b. Fault diagnosis of rolling element bearing based on symmetric cross entropy of neutrosophic sets. *Measurement* 152, 107318. <https://doi.org/10.1016/j.measurement.2019.107318>
- [14] Zadeh, L.A. (1965), "Fuzzy sets", *Information and control*, 8, p.338-353.
- [15] Bhandari, D. and Pal, N.R. (1993), "Some new information measures for fuzzy sets", *Information Sciences*, 67, p.209-226.
- [16] Shang, X.G., Jiang, W.S. (1997), "A note on fuzzy information measures", *Pattern Recognition Letters*, 18, p.425-432.

Received: Dec. 5, 2021. Accepted: April 3, 2022.